

# We are IntechOpen, the world's leading publisher of Open Access books Built by scientists, for scientists

4,800

Open access books available

122,000

International authors and editors

135M

Downloads

Our authors are among the

154

Countries delivered to

TOP 1%

most cited scientists

12.2%

Contributors from top 500 universities



WEB OF SCIENCE™

Selection of our books indexed in the Book Citation Index  
in Web of Science™ Core Collection (BKCI)

Interested in publishing with us?  
Contact [book.department@intechopen.com](mailto:book.department@intechopen.com)

Numbers displayed above are based on latest data collected.  
For more information visit [www.intechopen.com](http://www.intechopen.com)



# Graphene-Based Heterogeneous Electrodes for Energy Storage

*Ning Wang, Haixu Wang, Guang Yang, Rong Sun  
and Ching-Ping Wong*

## Abstract

As an intriguing two dimensional material, graphene has attracted intense interest due to its high stability, large carrier mobility as well as the excellent conductivity. The addition of graphene into the heterogeneous electrodes has been proved to be an effective method to improve the energy storage performance. In this chapter, the latest graphene based heterogeneous electrodes will be fully reviewed and discussed for energy storage. In detail, the assembly methods, including the ball-milling, hydrothermal, electrospinning, and microwave-assisted approaches will be illustrated. The characterization techniques, including the x-ray diffraction, scanning electron microscopy, transmission electron microscopy, electrochemical impedance spectroscopy, atomic force microscopy, and x-ray photoelectron spectroscopy will also be presented. The mechanisms behind the improved performance will also be fully reviewed and demonstrated. A conclusion and an outlook will be given in the end of this chapter to summarize the recent advances and the future opportunities, respectively.

**Keywords:** graphene, heterogeneous electrode, energy storage, hydrothermal, EIS, XPS

## 1. Introduction

In order to overcome the exhaustion of fossil fuels and to address the ever-growing demands for clean, sustainable and high efficient energy supply [1–3], the advanced energy storage techniques, including the supercapacitors, rechargeable batteries (Li-ion battery (LIB), Na-ion battery (SIB)), fuel cells as well as the solar cells have been widely investigated for the commercial use [4–6]. In the advanced energy storage devices, especially for the rechargeable batteries, the electrode materials should have the following features: high energy density, high working voltage, high power density, long cycling stability, high rate capacity as well as the environmental friendly [7–10].

In the rechargeable batteries, e.g. LIBs, the commercial anode material is graphite, whose theoretical-specific capacity is only 372 mA h/g [10], which cannot meet the requirement of the advanced energy storage techniques as described above. In order to overcome the low specific capacity of the graphite anode, amounts of substitute anode materials, e.g. Si (4200 mAh/g) [11], SnO (790 mAh/g) [12, 13], SnSb (825 mAh/g) [14, 15], Sn (993 mAh/g) [16], SbS<sub>3</sub> (947 mAh/g) [17], have been developed for high-capacity rechargeable batteries (**Figure 1**). However, the cycling stability became the most challenging issue for the high-capacity anode materials

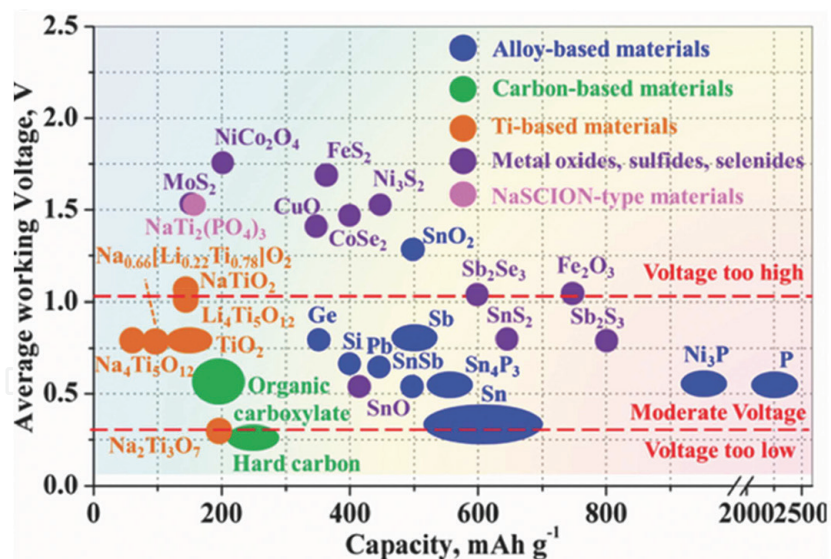


**Figure 1.**

Performance data of anode materials for SIB, reproduced with permission [19].

due to the volume expansion along with the charge–discharge process [18], e.g. 320% expansion for Si anode. Therefore, the gradient and/or the heterostructured anode materials could be the alternative approaches for the long cycling-stability, high specific capacity rechargeable batteries.

As a promising two dimensional (2D) material, graphene has attracted intense interest in the field of transparent electrode [20–24], field emission transistors (FET) [25–27], flexible devices [28–31], corrosion protection [32–34], catalysis [35–37] and energy storage [38–40], due to its large electrical conductivity, high thermal/chemical stability as well as the flexibility. With respect to the electrode materials, the graphene based heterogeneous electrodes were expected to occupy the excellent electrical conductivity, the long cycling stability and the high rate capability.

In this chapter, the assembly strategies for the graphene based heterogeneous electrodes, including the ball-milling, hydrothermal, electrospinning, microwave-assisted approaches, and the characterization methods will be fully reviewed. The mechanism behind the enhanced performance with graphene will be discussed, and an outlook on the challenges that should be addressed in the future will also be illustrated in the end.

## 2. Strategies for the assembly

### 2.1 Ball-milling

As a low-temperature alloying method, ball-milling is highly efficient in preparing the alloys and composites [41–46]. As for the graphene based heterogeneous electrode materials, ball milling exhibited the advantages in the size/layer reduction [47], interface-contact enhancement [48, 49] as well as the low cost and time saving [50].

As illustrated by Tie et al. [47], in the ball milling preparation of Si@SiO<sub>x</sub>/graphene heterogeneous anode material (**Figure 2**), the graphene nanosheets (GNS) could be exfoliated from the expanded graphite (EG) due to the accumulated mechanical shearing force of the agate balls, and the particle size of silicon could be reduced to 50–100 nm, which contributed to the uniform dispersion of Si nanoparticles on the GNS, and finally gave rise to the Si@SiO<sub>x</sub>/graphene composite. Owing to the reduced Si nanoparticle size, the SiO<sub>x</sub> adhesion layer as well as the synergistic

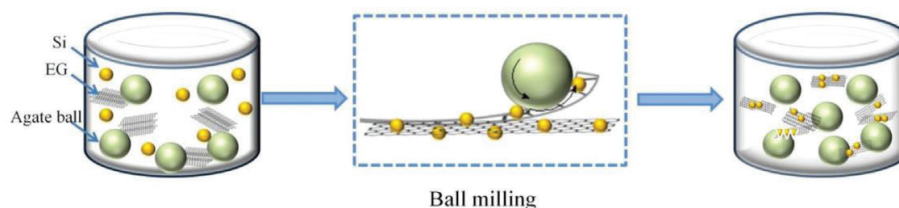


**Figure 2.** Schematic illustration for ball milling synthesis of Si@SiO<sub>x</sub>/graphene anode material [47].

effect of GNS, the Si@SiO<sub>x</sub>/graphene heterogeneous anode material exhibited the enhanced cycling stability, high reversible capacity, and rate capability.

Besides, the ball milling method could also be used to prepare other graphene based anode materials. Sun et al. [48] reported the ball milling synthesis of MoS<sub>2</sub>/graphene anode materials used for high rate SIBs, where the bulky MoS<sub>2</sub> and graphite were firstly expanded by the intercalation of Na<sup>+</sup> and K<sup>+</sup> between the layers, and then the several-layer MoS<sub>2</sub> nanosheets and the graphene sheets could be exfoliated from the loose counterparts, which finally resulted in the formation of the restacked MoS<sub>2</sub>/graphene heterostructures owing to the high surface energy and the interlayer Van der Waals attractions. Chen et al. [51] prepared the center-iodized graphene (CIG) and edge-iodized graphene (EIG) through the ball milling method, and the CIG were found to be an advanced anode material to boost the performance of the LIBs. In the other cases, Xia et al. [52] assembled the layer-by-layered SnS<sub>2</sub>/graphene anode materials for the LIBs via ball-milling, where the volume change of SnS<sub>2</sub> could be buffered by the graphene, and the shuttle effect in the cycling could also be suppressed, both of which gave rise to an excellent rate capability and the negligible capacity fading over 180 cycles; Ma et al. [49] prepared the MoTe<sub>2</sub>/FLG (few-layer graphene) anode material for the LIBs through the ball milling of MoTe<sub>2</sub> and graphite, which exhibited a high reversible capacity and an ultrahigh cycling stability.

## 2.2 Hydrothermal assembly

Hydrothermal method is an efficient and cost-effective approach for the assembly of metastable crystalline structures [53–57], especially for the heterogeneous structure with solid interface contact [58–61]. As for the graphene based heterogeneous electrode materials, the use of hydrothermal assembly could effectively reduce the cost, improve the crystallinity, and consolidate the interface contact, and therefore improve the energy storage performance.

Pang et al. [62] reported the hydrothermal assembly of VS<sub>4</sub>@GS (graphene sheets) nanocomposites used as the anode material for the SIBs. As shown in **Figure 3**, the CTA<sup>+</sup> (hexadecyl trimethyl ammonium ion) cations were firstly absorbed on the negatively charged GO (graphene oxide) sheets, and then the TAA (thioacetamide) and VO<sub>4</sub><sup>3-</sup> were attached onto the CTA<sup>+</sup> to form the TAA-VO<sub>4</sub><sup>3-</sup>-CTA<sup>+</sup>-GO complex, which was then transferred into the VS<sub>4</sub>/GS composite under the hydrothermal conditions. As an anode material, this composite exhibited a large specific capacity, good rate capability, and remarkable long cycling stability, which should be ascribed to the porous structure together with the synergistic interaction between the highly conductive graphene network and the VS<sub>4</sub> nanoparticles.

In other cases, hydrothermal assembly could also be used to fabricate the polyaniline (PANI)/graphene [58, 63], TiO<sub>2</sub>/graphene [64], Mn<sub>3</sub>O<sub>4</sub>/CeO<sub>2</sub>/graphene [65], α-Fe<sub>2</sub>O<sub>3</sub>/graphene [59], and Mn<sub>3</sub>O<sub>4</sub>/graphene electrode materials [66]. As illustrated in the literatures, the hydrothermal assembly of graphene based heterogeneous electrode materials is usually starting with the graphite oxide (GO), the active electrode materials and/or surfactants, which should be

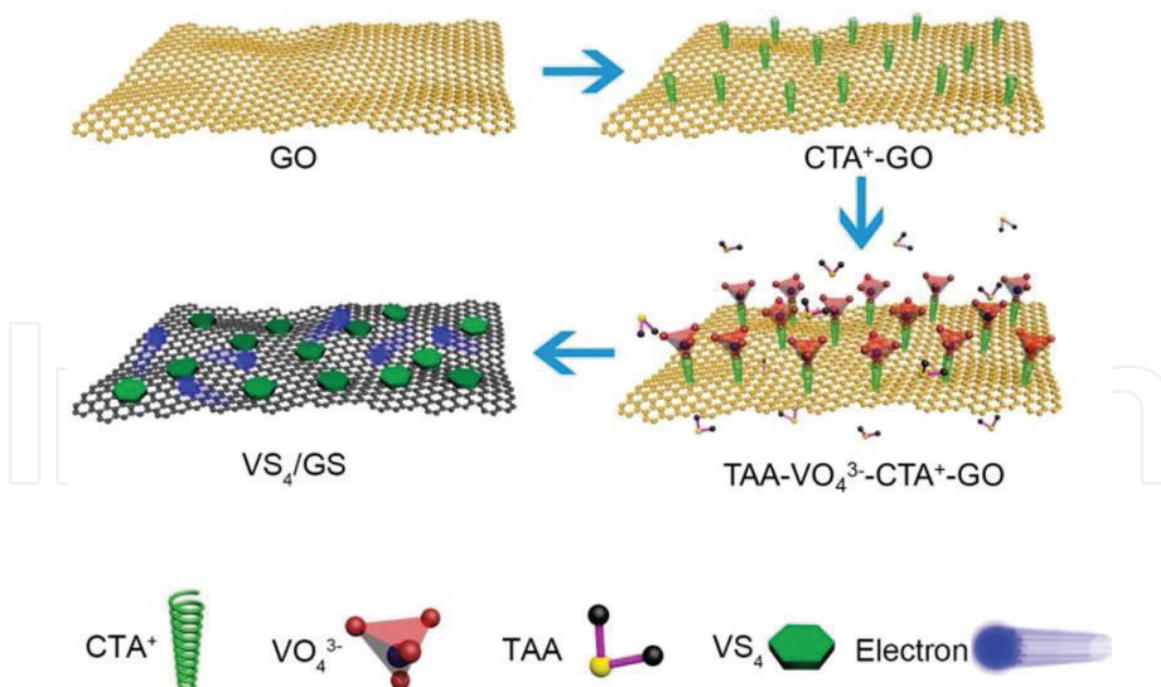


**Figure 3.**  
Hydrothermal synthesis route for the  $VS_4@GS$  nanocomposites [62].

mainly due to the intrinsic negatively charged surface of the GO that could be easily attached to the positively charged surfactants, and facilitate the nucleation and the growth of active materials on the reduced graphite oxide (rGO, graphene) sheets under the hydrothermal conditions. The strong interface adhesion and the high crystallinity of the hydrothermal assembled composite should benefit the electrode with improved energy storage performance.

### 2.3 Electrospinning

As an efficient fabrication method for nanofibers [67–73], the electrospinning method has also been developed for producing nanofiber/graphene heterogeneous electrode materials for the energy storage applications [74–78].

As an example, Wei et al. [78] demonstrated an electrospinning fabrication of GO-PAN/PVDF (GPP) membrane electrode for fuel cell applications. In the preparation of GPP membrane electrode material (**Figure 4**), the uniform GPP precursor was prepared by dispersing the PAN, PVDF, and GO in DMF solvent, and then the GPP nanofibers were coated onto the carbon paper sheet attached on a collector drum via the electrospinning. Finally, the electrode was assembled by loading the Pt/C catalysts on the GPP nanofiber membranes.

As a promising procedure, the electrospinning method was also reported to prepare the carbon nanofibers [74], carbonized gold (Au)/graphene (G) hybrid nanowires [75], GO/PVA composite nanofibers [76], and graphene/carbon nanofibers [77] electrode materials for the supercapacitor, biosensor applications. It should be noticed that the uniformity and the viscosity of the precursor should be carefully controlled, since both of which are critical for the mechanical strength and the electrochemical performance of the ultimate products.

### 2.4 Microwave-assisted assembly

As a quick and even heating method throughout the sample, the microwave assisted heating method has been widely used in the preparation of nanomaterials [79, 80].

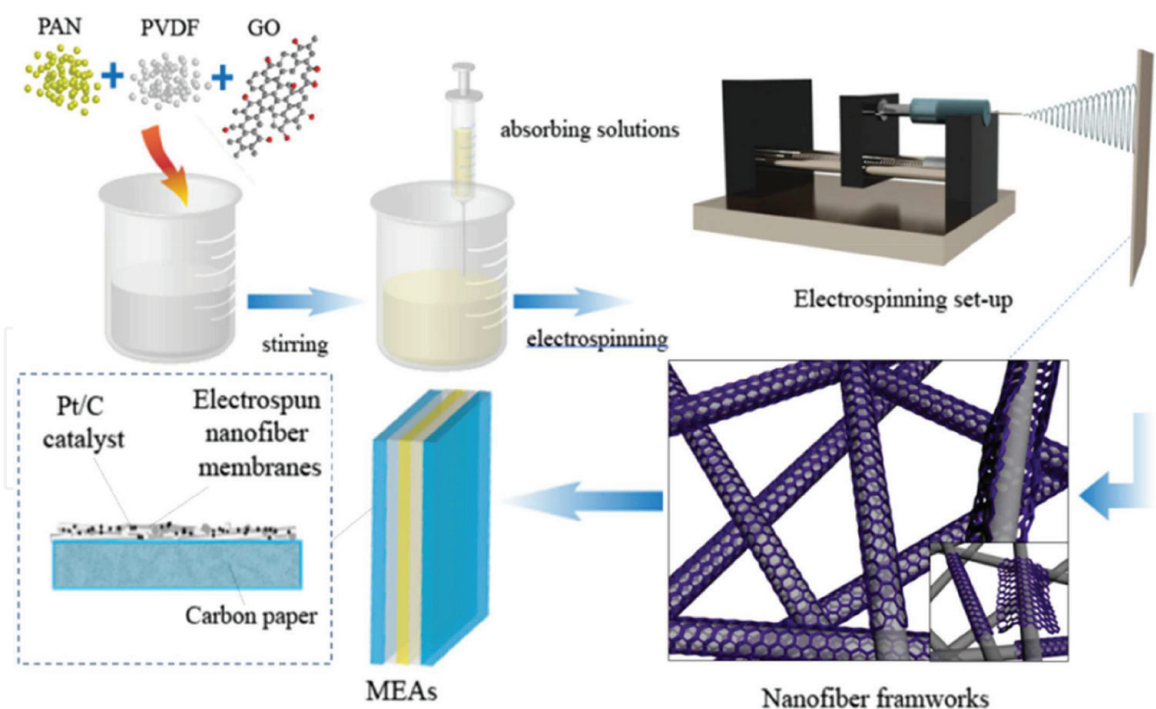


**Figure 4.** A synthetic route to GO-PAN/PVDF (GPP) nanofibers [78]. PAN is polyacrylonitrile, and PVDF is polyvinylidene fluoride.

In the preparation of graphene based electrode materials, the microwave assisted method has shown the advantages in the reduction and exfoliation of GO, the time efficiency, and the energy saving [9, 81–83].

As shown in **Figure 5**, Kumar et al. [81] reported the microwave assisted synthesis of palladium (Pd) nanoparticle intercalated nitrogen doped rGO (NrGO) and the application as anode material for the fuel cells. In this synthesis, the GO nanosheets could be reduced and exfoliated under the microwave irradiation with pyridine treatment, and the nitrogen doping could also be achieved via the further

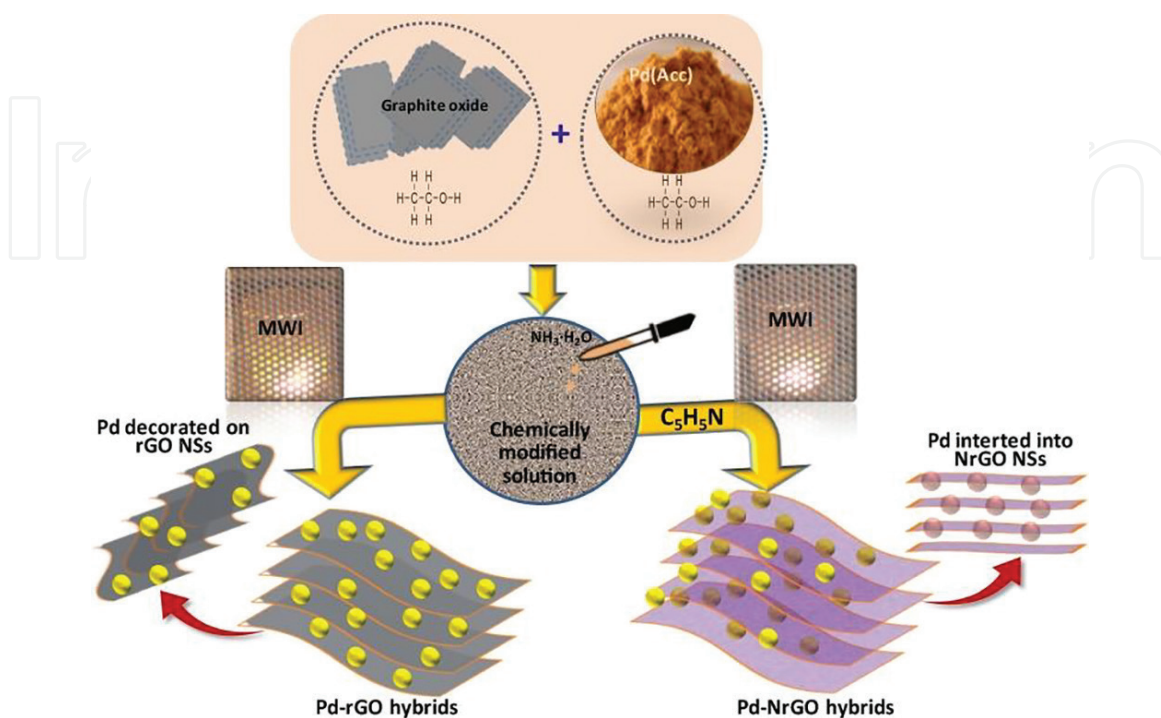


**Figure 5.** Schematic illustration of the microwave assisted synthesis of Pd-rGO and Pd-NrGO hybrids [81].

modification with pyridine. The obtained porous rGO and NrGO could be decorated with Pd nanoparticles, which gave rise to a high electroactive surface, and therefore resulted in a high catalytic activity.

For the energy storage electrode materials, the microwave assisted method has been used to ultrafast assembly of the  $Mn_{0.8}Co_{0.2}CO_3$ /graphene composite [9],  $SnO_2$ /graphene composite for LIBs [82], and  $SnO_2$ @graphene/N-doped carbons for SIBs [83]. The ultrafast and uniform heating effect of the microwave method should be due to the dielectric heating principle, under which the polar molecules in the microwave radiation could rotate in a high frequency, and thus generate thermal energies evenly across the samples, which benefits the synthesis with environmental friendship, low cost, low energy consumption as well as the porous structures that especially provide the quick transfer channels of the  $Li^+/Na^+$  cations in the rechargeable batteries.

### 3. Characterization methods

#### 3.1 Scanning electron microscopy (SEM)

In the morphology analysis of the graphene based heterogeneous electrode materials, the top-view and cross-section SEM (**Figure 6**) could be used to determine the distribution of the active materials wrapped or attached by the layered graphene substrates based on the high resolution detector for the secondary electrons emitted on the sample surface. Combined with the EDS (energy dispersive X-ray spectroscopy) technique, the interface of the heterogeneous electrode could also be figured out clearly via the elemental mapping for the active materials and the graphene substrates [48, 51, 82].

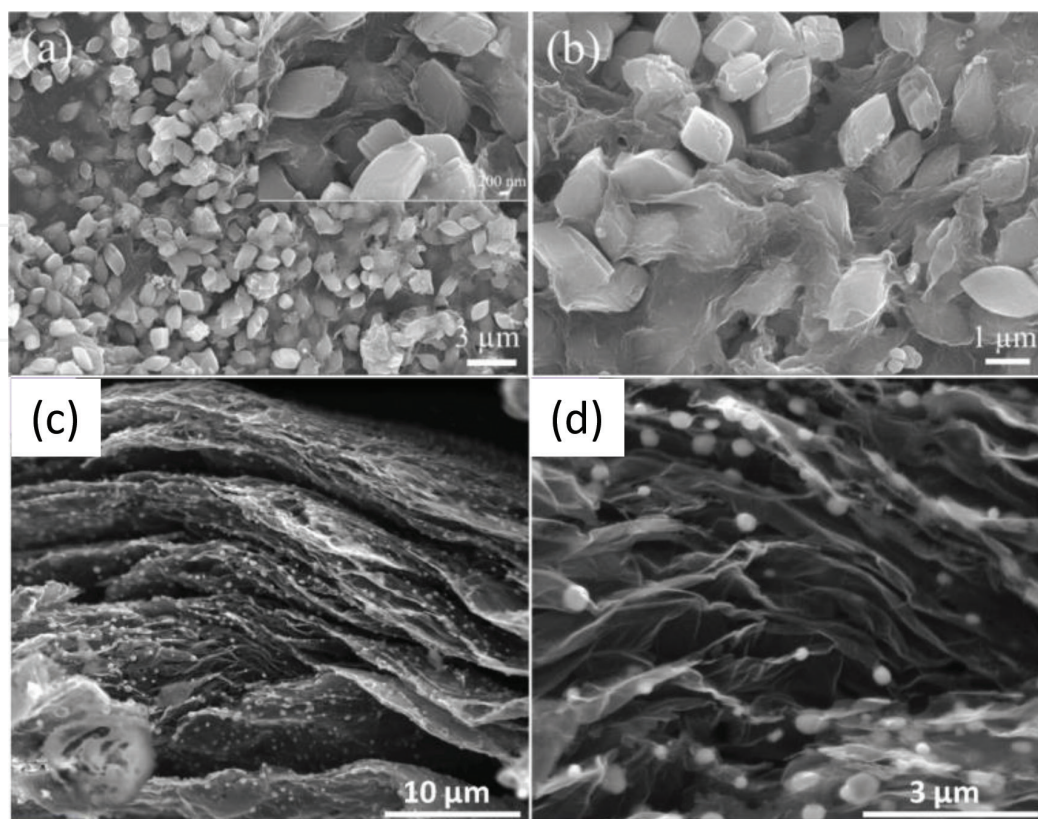


**Figure 6.** SEM images for the  $Mn_{0.8}Co_{0.2}CO_3$ /graphene oxide (a, b) [9] and Pd-NrGO hybrids (c, d) [81].

### 3.2 Transmission electron microscopy (TEM)

As a powerful characterization method, TEM has been widely used to determine the morphology, crystal structure as well as the interface adhesion of the heterogeneous structures due to its atomic level resolution and the sensitivity to the contrast changes along with the elemental differences on the interface [84, 85]. With respect to the graphene based heterogeneous electrode materials, as shown in **Figure 7**, the uniform dispersion of SnO<sub>2</sub> on the graphene layers could be determined in the low magnification TEM image (**Figure 7b, c**), and the well crystallized SnO<sub>2</sub> nanoparticles could be clearly indexed in the HRTEM (high resolution transmission electron microscopy) and the corresponding FFT (Fast Fourier Transform) patterns (**Figure 7d–i**). The morphology and the crystal structure determined by TEM should be consistent with the result of SEM and XRD, respectively.

### 3.3 X-ray photoelectron spectroscopy (XPS)

X-ray photoelectron spectroscopy (XPS) is a promising technique for determining the stoichiometry, the valence states, and the bonding conditions of the elements in the compounds, which has been widely used to characterize the functional materials [86–90]. Regarding to the graphene based heterogeneous electrode materials, as shown in **Figure 8** for the high resolution XPS scan of Pd-NrGO hybrids [81], the C 1s XPS peak could be split into the peaks for C=C (284.6 eV), C–O (286.4 eV), C–N

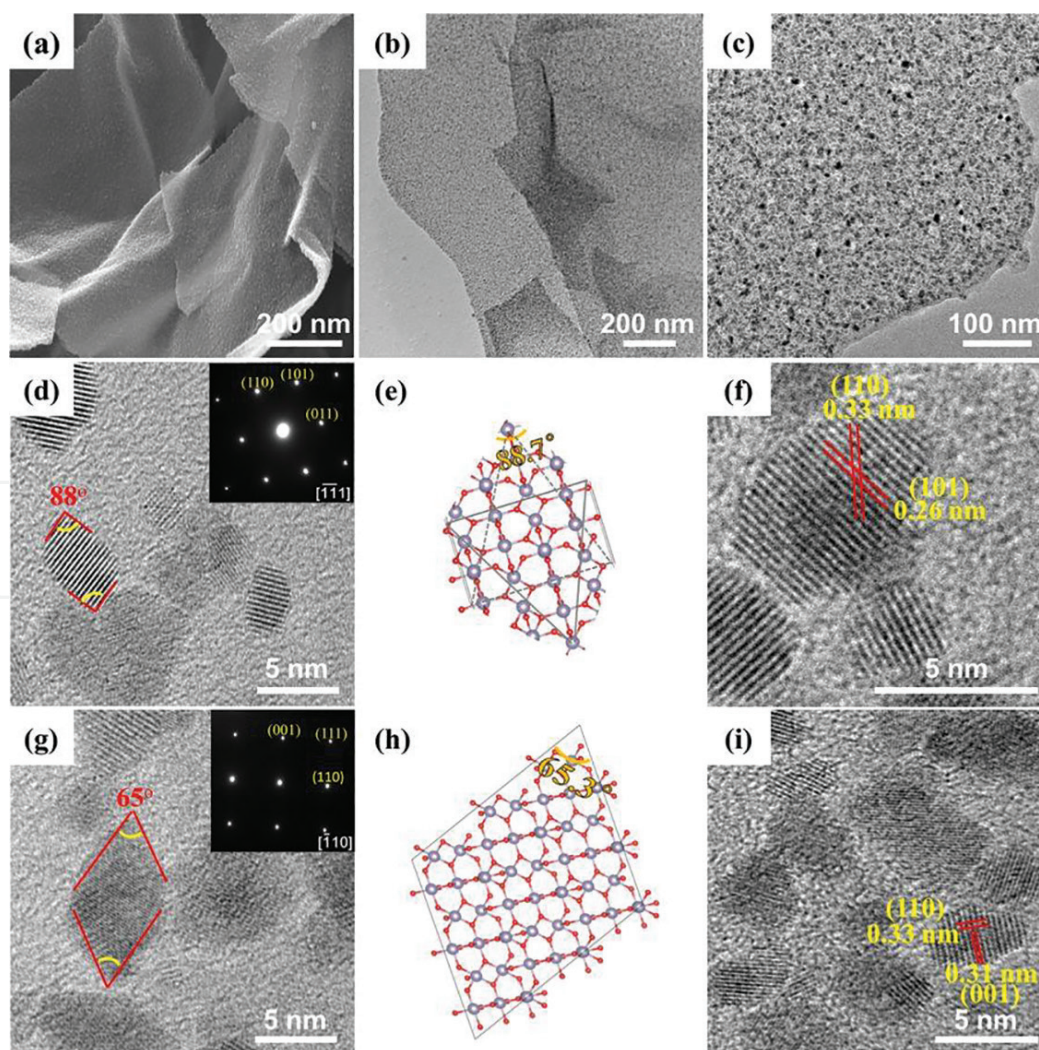


**Figure 7.** (a) SEM image. (b, c) Low-magnification TEM images for the SnO<sub>2</sub>/graphene hybrids. HRTEM images showing the octahedral SnO<sub>2</sub> model enclosed by {221} facets with (d–f)  $[\bar{1}\bar{1}1]$  and (g–i)  $[\bar{1}01]$  zone axes [7].

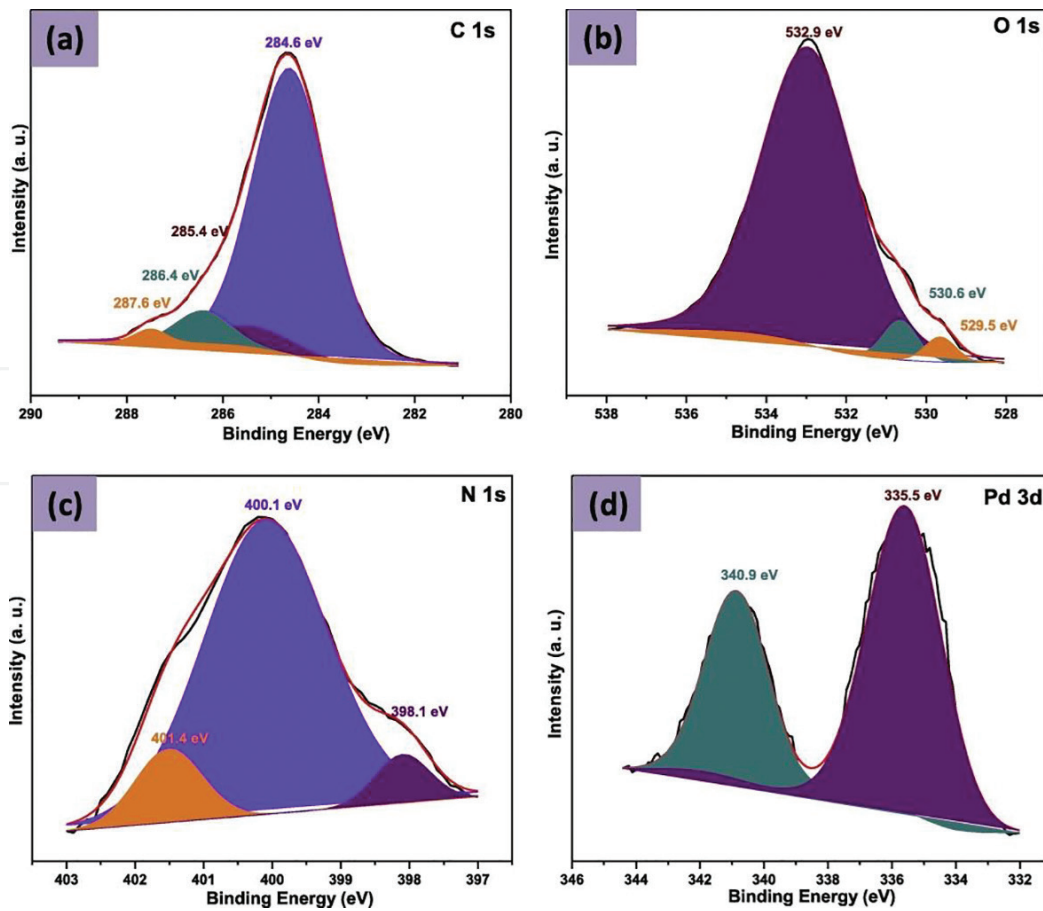


**Figure 8.** High resolution XPS spectra for (a) C 1s, (b) O 1s, (c) N 1s and (d) Pd 3d of Pd-NrGO hybrids [81].

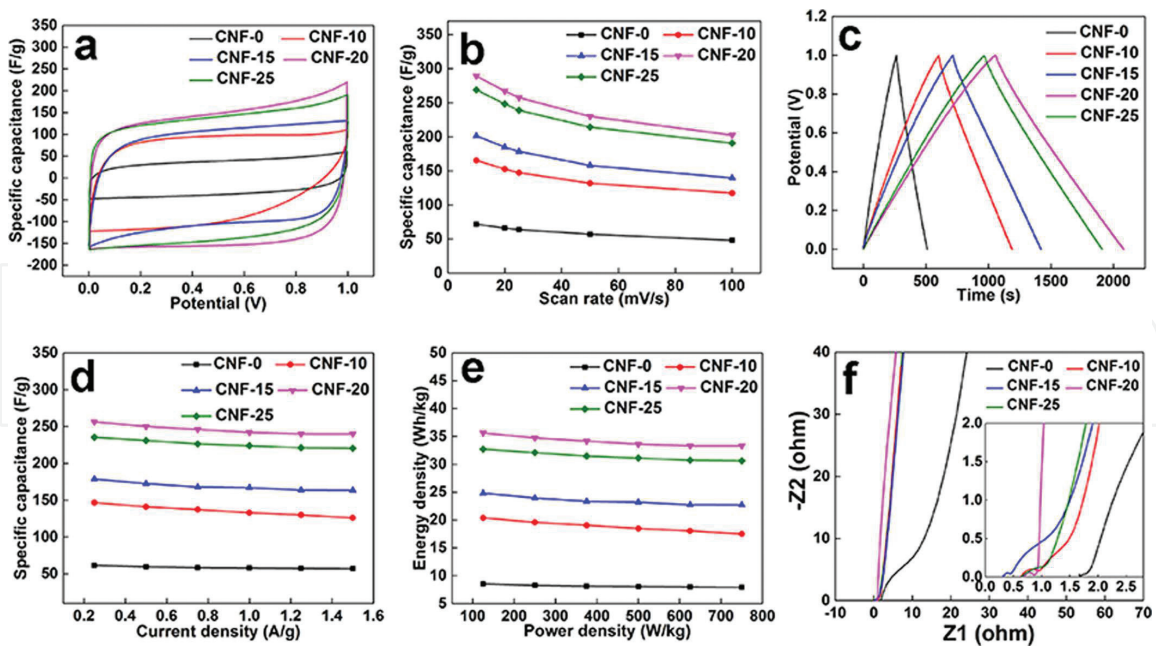


**Figure 9.** (a) Cyclic voltammetry (CV) curves of carbon nanofiber samples, (b) rate capability curves of carbon nanofiber from 10 to 100 mV/s, (c) GCD curves of carbon nanofiber samples, (d) rate capability curves of carbon nanofiber from 0.25 to 1.5 A/g, (e) Ragone plots of the supercapacitor devices, and (f) Nyquist plots of carbon nanofiber samples [74].

(285.4 eV), and C=N (287.6 eV), the N 1S peak could be split into the graphitic-N (401.4 eV), pyrrolic-N (400.1 eV) and pyridinic-N (398.1 eV) peaks, and the O 1S could be split into the Pd–O (529.5 eV), C–O (530.6 eV), and C=O (532.9 eV) peaks, which fully revealed the bonding information within the Pd-NrGO hybrids.

Apart from the SEM, TEM, and XPS, X-ray diffraction (XRD), Raman, FTIR, and thermal analysis methods (TGA, DSC) were also used to determine the crystal structure, morphology, thermal stability, and other physical/chemical characteristics of the graphene based heterogeneous electrode materials. The electrochemical performance for the energy storage was usually evaluated by the tests, including the cyclic voltammetry (CV), rate capability, galvanostatic charge/discharge (GCD), cycling specific capacity, and the electrochemical impedance spectra (EIS, e.g. Nyquist plots) (**Figure 9**).

#### 4. Mechanisms

As for the active materials in the anode for the energy storage devices (e.g. supercapacitor, LIBs, and SIBs), the modification via bonding or attaching with the graphene or rGO always results in the improvement of the electrochemical performance with respect to the cycling stability, rate capability as well as the high specific capacity.

Behind the enhancement of the performance, there exist several possible mechanisms for the property promotion as illustrated in the following:

- a. The growth of nanoparticles for the active materials could be effectively restricted by the graphene, giving rise to the uniform dispersion of the nanoparticles that facilitates the increase of specific area and the active sites for  $K^+/Na^+$  storage [7].
- b. The non-faradaic capacitance could be contributed by the graphene due to the electrical double layer-effect [7].
- c. The fragmentation of the active materials due to the volume expansion and contraction during the charge–discharge cycles could be depressed by the flexible graphene, which benefits the devices with excellent cycling stability and rate capability [7, 52].
- d. The conductivity of the active materials could be enhanced by the graphene, which gives rise to the increase of reversible capacity [52].
- e. The graphene in the composite could supply a physical barrier between the active materials and the electrolyte, which effectively suppresses the shuttle effect of the byproducts in the de-charge process that could fade capacity of the batteries [52].

#### 5. Conclusions and outlook

In summary, the synthesis and the characterization of the graphene based heterogeneous electrode materials for the energy storage applications (e.g. SIBs, LIBs, and supercapacitor) have been fully reviewed and discussed in this chapter. In the synthesis of the title materials, ball milling and hydrothermal methods show the cost-effective advantages. Comparatively, the electrospinning method exhibits the benefits in the nanowire composite assembly, and the microwave assisted approach occupies the superiority in the ultrafast fabrication. With respect to the characterization, the morphology could be determined by the SEM and TEM, and the electrochemical performance could be evaluated by the cyclic voltammetry (CV), rate capability, galvanostatic charge/ discharge (GCD), cycling specific capacity, and the EIS tests. In the composite, the graphene could restrict the growth of the nanosized active materials, contribute the non-faradaic capacitance, improve the conductivity, suppress the fragmentation, and supply a physical barrier between the active materials and the electrolyte, which benefit the devices with excellent cycling stability, large rate capability as well as the high specific capacity.

In the future, the most interesting and challenging applications of the graphene in the nanocomposite for the energy storage devices should be the ultrafast rechargeable batteries, the large-energy-density supercapacitors, and the all-solid-state LIBs.

## Acknowledgements

This work was supported by the National Key R&D Project from Minister of Science and Technology of China (No. 2017YFB0406200), National and Local Joint Engineering Laboratory of Advanced Electronic Packaging Materials (Shenzhen Development and Reform Committee 2017-934), Leading Scientific Research Project of Chinese Academy of Sciences(QYZDY-SSW-JSC010), and Guangdong Provincial Key Laboratory (2014B030301014).

## Conflict of interest

The authors declare no conflict of interest.

## Acronyms and abbreviations

LIBs	lithium ion batteries
SIBs	sodium ion batteries
SEM	scanning electron microscopy
TEM	transmission electron microscopy
XRD	X-ray diffraction
XPS	X-ray photoelectron spectroscopy
FTIR	Fourier-transform infrared spectroscopy
TGA	thermal gravimetric analysis
DSC	differential scanning calorimetry

IntechOpen

## Author details

Ning Wang\*, Haixu Wang, Guang Yang, Rong Sun and Ching-Ping Wong  
Shenzhen Institutes of Advanced Technology, Chinese Academy of Sciences,  
Shenzhen, China

\*Address all correspondence to: ning.wang@siat.ac.cn

## IntechOpen

© 2018 The Author(s). Licensee IntechOpen. This chapter is distributed under the terms of the Creative Commons Attribution License (<http://creativecommons.org/licenses/by/3.0>), which permits unrestricted use, distribution, and reproduction in any medium, provided the original work is properly cited. 

## References

- [1] Dunn B, Kamath H, Tarascon J-M. Electrical energy storage for the grid: A battery of choices. *Science*. 2011;**334**:928-935. DOI: 10.1126/science.1212741
- [2] Choi JW, Aurbach D. Promise and reality of post-lithium-ion batteries with high energy densities. *Nature Reviews Materials*. 2016;**1**:16013. DOI: 10.1038/natrevmats.2016.13
- [3] Larcher D, Tarascon JM. Towards greener and more sustainable batteries for electrical energy storage. *Nature Chemistry*. 2014;**7**:19. DOI: 10.1038/nchem.2085
- [4] Slater Michael D, Kim D, Lee E, Johnson Christopher S. Sodium-ion batteries. *Advanced Functional Materials*. 2012;**23**:947-958. DOI: 10.1002/adfm.201200691
- [5] Nayak Prasant K, Yang L, Brehm W, Adelhelm P. From lithium-ion to sodium-ion batteries: Advantages, challenges, and surprises. *Angewandte Chemie International Edition*. 2017;**57**:102-120. DOI: 10.1002/anie.201703772
- [6] Sun Y, Liu N, Cui Y. Promises and challenges of nanomaterials for lithium-based rechargeable batteries. *Nature Energy*. 2016;**1**:16071. DOI: 10.1038/nenergy.2016.71
- [7] Zhang P, Zhao X, Liu Z, Wang F, Huang Y, Li H, Li Y, Wang J, Su Z, Wei G. Exposed high-energy facets in ultradispersed sub-10 nm SnO<sub>2</sub> nanocrystals anchored on graphene for pseudocapacitive sodium storage and high-performance quasi-solid-state sodium-ion capacitors. *NPG Asia Materials*. 2018;**10**:429-440. DOI: 10.1038/s41427-018-0049-y
- [8] Zhang J, Li JY, Wang WP, Zhang XH, Tan XH, Chu WG, Guo YG. Microemulsion assisted assembly of 3D porous S/graphene@ g-C<sub>3</sub>N<sub>4</sub> hybrid sponge as free-standing cathodes for high energy density Li-S batteries. *Advanced Energy Materials*. 2018;**8**:1702839. DOI: 10.1002/aenm.201702839
- [9] Xiong Q, Lou J, Zhou Y, Shi S, Ji Z. Ultrafast synthesis of Mn<sub>0.8</sub>Co<sub>0.2</sub>CO<sub>3</sub>/graphene composite as anode material by microwave solvothermal strategy with enhanced Li storage properties. *Materials Letters*. 2018;**210**:267-270. DOI: 10.1016/j.matlet.2017.09.045
- [10] Wang G, Zhang J, Yang S, Wang F, Zhuang X, Müllen K, Feng X. Vertically aligned MoS<sub>2</sub> nanosheets patterned on electrochemically exfoliated graphene for high-performance lithium and sodium storage. *Advanced Energy Materials*. 2018;**8**:1702254. DOI: 10.1002/aenm.201702254
- [11] Chan CK, Peng H, Liu G, McIlwrath K, Zhang XF, Huggins RA, Cui Y. High-performance lithium battery anodes using silicon nanowires. *Nature Nanotechnology*. 2007;**3**:31. DOI: 10.1038/nnano.2007.411
- [12] Aurbach D, Nimberger A, Markovsky B, Levi E, Sominski E, Gedanken A. Nanoparticles of SnO produced by sonochemistry as anode materials for rechargeable lithium batteries. *Chemistry of Materials*. 2002;**14**:4155-4163. DOI: 10.1021/cm021137m
- [13] Kim H, Cho J. Hard templating synthesis of mesoporous and nanowire SnO<sub>2</sub> lithium battery anode materials. *Journal of Materials Chemistry*. 2008;**18**:771-775. DOI: 10.1039/b714904b
- [14] Chao S-C, Song Y-F, Wang C-C, Sheu H-S, Wu H-C, Wu N-L. Study on microstructural deformation of working

- Sn and SnSb anode particles for Li-ion batteries by in situ transmission X-ray microscopy. *The Journal of Physical Chemistry C*. 2011;**115**:22040-22047. DOI: 10.1021/jp206829q
- [15] Shi L, Li H, Wang Z, Huang X, Chen L. Nano-SnSb alloy deposited on MCMB as an anode material for lithium ion batteries. *Journal of Materials Chemistry*. 2001;**11**:1502-1505. DOI: 10.1039/b009907o
- [16] Deng D, Kim MG, Lee JY, Cho J. Green energy storage materials: Nanostructured TiO<sub>2</sub> and Sn-based anodes for lithium-ion batteries. *Energy & Environmental Science*. 2009;**2**:818-837. DOI: 10.1039/b823474d
- [17] Xiong X, Wang G, Lin Y, Wang Y, Ou X, Zheng F, Yang C, Wang J-H, Liu M. Enhancing sodium ion battery performance by strongly binding nanostructured Sb<sub>2</sub>S<sub>3</sub> on sulfur-doped Graphene sheets. *ACS Nano*. 2016;**10**:10953-10959. DOI: 10.1021/acsnano.6b05653
- [18] Yao Y, McDowell MT, Ryu I, Wu H, Liu N, Hu L, Nix WD, Cui Y. Interconnected silicon hollow nanospheres for Lithium-ion battery anodes with long cycle life. *Nano Letters*. 2011;**11**:2949-2954. DOI: 10.1021/nl201470j
- [19] Xu GL, Amine R, Abouimrane A, Che H, Dahbi M, Ma ZF, Saadoune I, Alami J, Mattis Wenjuan L, Pan F, Chen Z, Amine K. Challenges in developing electrodes, electrolytes, and diagnostics tools to understand and advance sodium-ion batteries. *Advanced Energy Materials*. 2018;**0**:1702403. DOI: 10.1002/aenm.201702403
- [20] Wu J, Becerril HA, Bao Z, Liu Z, Chen Y, Peumans P. Organic solar cells with solution-processed graphene transparent electrodes. *Applied Physics Letters*. 2008;**92**:263302. DOI: 10.1063/1.2924771
- [21] Bae S, Kim H, Lee Y, Xu X, Park J-S, Zheng Y, Balakrishnan J, Lei T, Ri Kim H, Song YI, Kim Y-J, Kim KS, Özyilmaz B, Ahn J-H, Hong BH, Iijima S. Roll-to-roll production of 30-inch graphene films for transparent electrodes. *Nature Nanotechnology*. 2010;**5**:574. DOI: 10.1038/nnano.2010.132
- [22] Kim KS, Zhao Y, Jang H, Lee SY, Kim JM, Kim KS, Ahn J-H, Kim P, Choi J-Y, Hong BH. Large-scale pattern growth of graphene films for stretchable transparent electrodes. *Nature*. 2009;**457**:706. DOI: 10.1038/nature07719
- [23] Wu J, Agrawal M, Becerril HA, Bao Z, Liu Z, Chen Y, Peumans P. Organic light-emitting diodes on solution-processed graphene transparent electrodes. *ACS Nano*. 2010;**4**:43-48. DOI: 10.1021/nn900728d
- [24] Pang S, Hernandez Y, Feng X, Müllen K. Graphene as transparent electrode material for organic electronics. *Advanced Materials*. 2011;**23**:2779-2795. DOI: 10.1002/adma.201100304
- [25] Lin Y-M, Dimitrakopoulos C, Jenkins KA, Farmer DB, Chiu H-Y, Grill A, Avouris P. 100-GHz transistors from wafer-scale epitaxial graphene. *Science*. 2010;**327**:662-662. DOI: 10.1126/science.1184289
- [26] Chen F, Xia J, Ferry DK, Tao N. Dielectric screening enhanced performance in graphene FET. *Nano Letters*. 2009;**9**:2571-2574. DOI: 10.1021/nl900725u
- [27] Fiori G, Iannaccone G. On the possibility of tunable-gap bilayer graphene FET. *IEEE Electron Device Letters*. 2009;**30**:261-264. DOI: 10.1109/led.2008.2010629
- [28] Cho B, Yoon J, Hahm MG, Kim D-H, Kim AR, Kahng YH, Park S-W, Lee Y-J, Park S-G, Kwon J-D, Kim CS, Song M,

- Jeong Y, Nam K-S, Ko HC. Graphene-based gas sensor: Metal decoration effect and application to a flexible device. *Journal of Materials Chemistry C*. 2014;**2**:5280-5285. DOI: 10.1039/c4tc00510d
- [29] Sumboja A, Foo Ce Y, Wang X, Lee Pooi S. Large areal mass, flexible and free-standing reduced graphene oxide/manganese dioxide paper for asymmetric supercapacitor device. *Advanced Materials*. 2013;**25**:2809-2815. DOI: 10.1002/adma.201205064
- [30] El-Kady MF, Strong V, Dubin S, Kaner RB. Laser scribing of high-performance and flexible graphene-based electrochemical capacitors. *Science*. 2012;**335**:1326-1330. DOI: 10.1126/science.1216744
- [31] Feng L, Wang K, Zhang X, Sun X, Li C, Ge X, Ma Y. Flexible solid-state supercapacitors with enhanced performance from hierarchically graphene nanocomposite electrodes and ionic liquid incorporated gel polymer electrolyte. *Advanced Functional Materials*. 2017;**28**:1704463. DOI: 10.1002/adfm.201704463
- [32] Glover CF, Richards CAJ, Williams G, McMurray HN. Evaluation of multi-layered graphene nano-platelet composite coatings for corrosion control part II—Cathodic delamination kinetics. *Corrosion Science*. 2018;**136**:304-310. DOI: 10.1016/j.corsci.2018.03.014
- [33] Lee J, Berman D. Inhibitor or promoter: Insights on the corrosion evolution in a graphene protected surface. *Carbon*. 2018;**126**:225-231. DOI: 10.1016/j.carbon.2017.10.022
- [34] Yu F, Camilli L, Wang T, Mackenzie DMA, Curioni M, Akid R, Bøggild P. Complete long-term corrosion protection with chemical vapor deposited graphene. *Carbon*. 2018;**132**:78-84. DOI: 10.1016/j.carbon.2018.02.035
- [35] Qiu B, Xing M, Zhang J. Recent advances in three-dimensional graphene based materials for catalysis applications. *Chemical Society Reviews*. 2018;**47**:2165-2216. DOI: 10.1039/c7cs00904f
- [36] Xi J, Wang Q, Liu J, Huan L, He Z, Qiu Y, Zhang J, Tang C, Xiao J, Wang S. N,P-dual-doped multilayer graphene as an efficient carbocatalyst for nitroarene reduction: A mechanistic study of metal-free catalysis. *Journal of Catalysis*. 2018;**359**:233-241. DOI: 10.1016/j.jcat.2018.01.003
- [37] Varela AS, Kroschel M, Leonard ND, Ju W, Steinberg J, Bagger A, Rossmeisl J, Strasser P. pH effects on the selectivity of the electrocatalytic CO<sub>2</sub> reduction on graphene-embedded Fe–N–C motifs: Bridging concepts between molecular homogeneous and solid-state heterogeneous catalysis. *ACS Energy Letters*. 2018;**3**:812-817. DOI: 10.1021/acsenenergylett.8b00273
- [38] Wang B, Ryu J, Choi S, Song G, Hong D, Hwang C, Chen X, Wang B, Li W, Song H-K, Park S, Ruoff RS. Folding graphene film yields high areal energy storage in lithium-ion batteries. *ACS Nano*. 2018;**12**:1739-1746. DOI: 10.1021/acsnano.7b08489
- [39] Geng P, Zheng S, Tang H, Zhu R, Zhang L, Cao S, Xue H, Pang H. Transition metal sulfides based on graphene for electrochemical energy storage. *Advanced Energy Materials*. 2018;**8**:1703259. DOI: 10.1002/aenm.201703259
- [40] Mao J, Iocozzia J, Huang J, Meng K, Lai Y, Lin Z. Graphene aerogels for efficient energy storage and conversion. *Energy & Environmental Science*. 2018;**11**:772-799. DOI: 10.1039/c7ee03031b
- [41] Lee J, Li Y, Tang JN, Cui XL. Synthesis of hydrogen substituted graphene through mechanochemistry

and its electrocatalytic properties.

Acta Physico-Chimica Sinica.

2018;**34**:1080-1087. DOI: 10.3866/Pku. Whxb201802262

[42] Fu X, Hu Y, Zhang T, Chen S. The role of ball milled h-BN in the enhanced photocatalytic activity: A study based on the model of ZnO. Applied Surface Science. 2013;**280**:828-835. DOI: 10.1016/j.apsusc.2013.05.069

[43] Fu X, Hu Y, Yang Y, Liu W, Chen S. Ball milled h-BN: An efficient holes transfer promoter to enhance the photocatalytic performance of TiO<sub>2</sub>. Journal of Hazardous materials. 2013;**244-245**:102-110. DOI: 10.1016/j.jhazmat.2012.11.033

[44] Fu X, Hu Y, Yang Y, Liu W, Chen S. Ball milled h-BN: An efficient holes transfer promoter to enhance the photocatalytic performance of TiO<sub>2</sub>. Journal of Hazardous Materials. 2013;**244-245**:102-110. DOI: 10.1016/j.jhazmat.2012.11.033

[45] Shkodich NF, Vadchenko SG, Nepapushev AA, Kovalev DY, Kovalev ID, Ruvimov S, Rogachev AS, Mukasyan AS. Crystallization of amorphous Cu<sub>50</sub>Ti<sub>50</sub> alloy prepared by high-energy ball milling. Journal of Alloys and Compounds. 2018;**741**:575-579. DOI: 10.1016/j.jallcom.2018.01.062

[46] Esquivel J, Wachowiak MG, O'Brien SP, Gupta RK. Thermal stability of nanocrystalline Al-5at.%Ni and Al-5at.%V alloys produced by high-energy ball milling. Journal of Alloys and Compounds. 2018;**744**:651-657. DOI: 10.1016/j.jallcom.2018.02.144

[47] Tie X, Han Q, Liang C, Li B, Zai J, Qian X. Si@SiO<sub>x</sub>/graphene nanosheets composite: Ball milling synthesis and enhanced lithium storage performance. Frontiers in Materials. 2018;**4**:47. DOI: 10.3389/fmats.2017.00047

[48] Sun D, Ye D, Liu P, Tang Y, Guo J, Wang L, Wang H. MoS<sub>2</sub>/graphene

nanosheets from commercial bulky MoS<sub>2</sub> and graphite as anode materials for high rate sodium-ion batteries. Advanced Energy Materials. 2017;**8**:1702383. DOI: 10.1002/aenm.201702383

[49] Ma N, Jiang XY, Zhang L, Wang XS, Cao YL, Zhang XZ. Novel 2D layered molybdenum ditelluride encapsulated in few-layer graphene as high-performance anode for lithium-ion batteries. Small. 2018;**14**:1703680. DOI: 10.1002/sml.201703680

[50] Sha L, Gao P, Ren X, Chi Q, Chen Y, Yang P. A self-repairing cathode material for Lithium-selenium batteries: Se-C chemically bonded selenium-graphene composite. Chemistry—A European Journal. 2018;**24**:2151-2156. DOI: 10.1002/chem.201704079

[51] Chen J, Xu M-W, Wu J, Li CM. Center-iodized graphene as an advanced anode material to significantly boost the performance of lithium-ion batteries. Nanoscale. 2018;**10**:9115-9122. DOI: 10.1039/c8nr00061a

[52] Xia J, Liu L, Xie J, Yan H, Yuan Y, Chen M, Huang C, Zhang Y, Nie S, Wang X. Layer-by-layered SnS<sub>2</sub>/graphene hybrid nanosheets via ball-milling as promising anode materials for lithium ion batteries. Electrochimica Acta. 2018;**269**:452-461. DOI: 10.1016/j.electacta.2018.03.022

[53] Zhu J, Zhou Y, Wang B, Zheng J, Ji S, Yao H, Luo H, Jin P. Vanadium dioxide nanoparticle-based thermochromic smart coating: High luminous transmittance, excellent solar regulation efficiency, and near room temperature phase transition. ACS Applied Materials & interfaces. 2015;**7**:27796-27803. DOI: 10.1021/acsami.5b09011

[54] Zhong L, Li M, Wang H, Luo Y, Pan J, Li G. Star-shaped VO<sub>2</sub> (M) nanoparticle films with high thermochromic performance. CrystEngComm. 2015;**17**:5614-5619. DOI: 10.1039/c5ce00873e

- [55] Zhang J, Jin H, Chen Z, Cao M, Chen P, Dou Y, Zhao Y, Li J. Self-assembling VO<sub>2</sub> nanonet with high switching performance at wafer-scale. *Chemistry of Materials*. 2015;**27**:7419-7424. DOI: 10.1021/acs.chemmater.5b03314
- [56] Zhang H, Li Q, Shen P, Dong Q, Liu B, Liu R, Cui T, Liu B. The structural phase transition process of free-standing monoclinic vanadium dioxide micron-sized rods: Temperature-dependent Raman study. *RSC Advances*. 2015;**5**:83139-83143. DOI: 10.1039/c5ra15947d
- [57] Powell MJ, Marchand P, Denis CJ, Bear JC, Darr JA, Parkin IP. Direct and continuous synthesis of VO<sub>2</sub> nanoparticles. *Nanoscale*. 2015;**7**:18686-18693. DOI: 10.1039/c5nr04444h
- [58] Wang R, Han M, Zhao Q, Ren Z, Guo X, Xu C, Hu N, Lu L. Hydrothermal synthesis of nanostructured graphene/polyaniline composites as high-capacitance electrode materials for supercapacitors. *Scientific Reports*. 2017;**7**:44562
- [59] Nathan DMGT, Bobby SJM. Hydrothermal preparation of hematite nanotubes/reduced graphene oxide nanocomposites as electrode material for high performance supercapacitors. *Journal of Alloys and Compounds*. 2017;**700**:67-74. DOI: 10.1016/j.jallcom.2017.01.070
- [60] Meng S, Ye X, Ning X, Xie M, Fu X, Chen S. Selective oxidation of aromatic alcohols to aromatic aldehydes by BN/metal sulfide with enhanced photocatalytic activity. *Applied Catalysis B: Environmental*. 2016;**182**:356-368. DOI: 10.1016/j.apcatb.2015.09.030
- [61] Alie D, Gedvilas L, Wang Z, Tenent R, Engtrakul C, Yan Y, Shaheen SE, Dillon AC, Ban C. Direct synthesis of thermochromic VO<sub>2</sub> through hydrothermal reaction. *Journal of Solid State Chemistry*. 2014;**212**:237-241. DOI: 10.1016/j.jssc.2013.10.023
- [62] Pang Q, Zhao Y, Yu Y, Bian X, Wang X, Wei Y, Gao Y, Chen G. VS<sub>4</sub> nanoparticles anchored on graphene sheets as a high-rate and stable electrode material for sodium ion batteries. *ChemSusChem*. 2018;**11**:735-742. DOI: 10.1002/cssc.201702031
- [63] Zou Y, Zhang Z, Zhong W, Yang W. Hydrothermal direct synthesis of polyaniline, graphene/polyaniline and N-doped graphene/polyaniline hydrogels for high performance flexible supercapacitors. *Journal of Materials Chemistry A*. 2018;**6**:9245-9256. DOI: 10.1039/c8ta01366g
- [64] Lee JS, You KH, Park CB. Highly photoactive, low bandgap TiO<sub>2</sub> nanoparticles wrapped by graphene. *Advanced Materials*. 2012;**24**:1084-1088. DOI: 10.1002/adma.201104110
- [65] Liu C, Sun H, Qian J, Chen Z, Chen F, Liu S, Lv Y, Lu X, Chen A. Ultrafine Mn<sub>3</sub>O<sub>4</sub>/CeO<sub>2</sub> nanorods grown on reduced graphene oxide sheets as high-performance supercapacitor electrodes. *Journal of Alloys and Compounds*. 2017;**722**:54-59. DOI: 10.1016/j.jallcom.2017.06.097
- [66] Lee JW, Hall AS, Kim J-D, Mallouk TE. A facile and template-free hydrothermal synthesis of Mn<sub>3</sub>O<sub>4</sub> nanorods on graphene sheets for supercapacitor electrodes with long cycle stability. *Chemistry of Materials*. 2012;**24**:1158-1164. DOI: 10.1021/cm203697w
- [67] Mantilaka MMMGPG, De Silva RT, Ratnayake SP, Amaratunga G, de Silva KMN. Photocatalytic activity of electrospun MgO nanofibres: Synthesis, characterization and applications. *Materials Research Bulletin*. 2018;**99**:204-210. DOI: 10.1016/j.materresbull.2017.10.047

- [68] Zhang L, Zhang Q, Xie H, Guo J, Lyu H, Li Y, Sun Z, Wang H, Guo Z. Electrospun titania nanofibers segregated by graphene oxide for improved visible light photocatalysis. *Applied Catalysis B: Environmental*. 2017;**201**:470-478. DOI: 10.1016/j.apcatb.2016.08.056
- [69] Han C, Mao W, Bao K, Xie H, Jia Z, Ye L. Preparation of Ag/Ga<sub>2</sub>O<sub>3</sub> nanofibers via electrospinning and enhanced photocatalytic hydrogen evolution. *International Journal of Hydrogen Energy*. 2017;**42**:19913-19919. DOI: 10.1016/j.ijhydene.2017.06.076
- [70] Zhang Y, Park M, Kim HY, Ding B, Park S-J. In-situ synthesis of nanofibers with various ratios of BiOCl<sub>x</sub>/BiOBr<sub>y</sub>/BiOI<sub>z</sub> for effective trichloroethylene photocatalytic degradation. *Applied Surface Science*. 2016;**384**:192-199. DOI: 10.1016/j.apsusc.2016.05.039
- [71] Zhang Y, Park M, Kim H-Y, El-Newehy M, Rhee KY, Park S-J. Effect of TiO<sub>2</sub> on photocatalytic activity of polyvinylpyrrolidone fabricated via electrospinning. *Composites Part B: Engineering*. 2015;**80**:355-360. DOI: 10.1016/j.compositesb.2015.05.040
- [72] Wang K, Shao C, Li X, Zhang X, Lu N, Miao F, Liu Y. Hierarchical heterostructures of p-type BiOCl nanosheets on electrospun n-type TiO<sub>2</sub> nanofibers with enhanced photocatalytic activity. *Catalysis Communications*. 2015;**67**:6-10. DOI: 10.1016/j.catcom.2015.03.037
- [73] Kayaci F, Vempati S, Ozgit-Akgun C, Donmez I, Biyikli N, Uyar T. Selective isolation of the electron or hole in photocatalysis: ZnO-TiO<sub>2</sub> and TiO<sub>2</sub>-ZnO core-shell structured heterojunction nanofibers via electrospinning and atomic layer deposition. *Nanoscale*. 2014;**6**:5735-5745. DOI: 10.1039/c3nr06665g
- [74] Wang H, Wang W, Wang H, Jin X, Niu H, Wang H, Zhou H, Lin T. High performance supercapacitor electrode materials from electrospun carbon nanofibers in situ activated by high decomposition temperature polymer. *ACS Applied Energy Materials*. 2018;**1**:431-439. DOI: 10.1021/acsaem.7b00083
- [75] Ekabutr P, Klinkajon W, Sangsanoh P, Chailapakul O, Niamlang P, Khampieng T, Supaphol P. Electrospinning: A carbonized gold/graphene/PAN nanofiber for high performance biosensing. *Analytical Methods*. 2018;**10**:874-883. DOI: 10.1039/c7ay02880f
- [76] Mishra RK, Nawaz MH, Hayat A, Nawaz MAH, Sharma V, Marty J-L. Electrospinning of graphene-oxide onto screen printed electrodes for heavy metal biosensor. *Sensors and Actuators B: Chemical*. 2017;**247**:366-373. DOI: 10.1016/j.snb.2017.03.059
- [77] Chee WK, Lim HN, Zainal Z, Harrison I, Andou Y, Huang NM, Altarawneh M, Jiang ZT. Electrospun graphene nanoplatelets-reinforced carbon nanofibers as potential supercapacitor electrode. *Materials Letters*. 2017;**199**:200-203. DOI: 10.1016/j.matlet.2017.04.086
- [78] Wei M, Jiang M, Liu X, Wang M, Mu S. Graphene-doped electrospun nanofiber membrane electrodes and proton exchange membrane fuel cell performance. *Journal of Power Sources*. 2016;**327**:384-393. DOI: 10.1016/j.jpowsour.2016.07.083
- [79] Schütz MB, Xiao L, Lehnen T, Fischer T, Mathur S. Microwave-assisted synthesis of nanocrystalline binary and ternary metal oxides. *International Materials Reviews*. 2018;**63**:341-374. DOI: 10.1080/09506608.2017.1402158
- [80] Zhong Y, Yu L, Chen Z-F, He H, Ye F, Cheng G, Zhang Q. Microwave-assisted synthesis of Fe<sub>3</sub>O<sub>4</sub> nanocrystals with predominantly exposed facets and their heterogeneous UVA/Fenton

- catalytic activity. *ACS Applied Materials & Interfaces*. 2017;**9**:29203-29212. DOI: 10.1021/acsami.7b06925
- [81] Kumar R, da Silva ET, Singh RK, Savu R, Alaferdov AV, Fonseca LC, Carossi LC, Singh A, Khandka S, Kar KK. Microwave-assisted synthesis of palladium nanoparticles intercalated nitrogen doped reduced graphene oxide and their electrocatalytic activity for direct-ethanol fuel cells. *Journal of Colloid and Interface Science*. 2018;**515**:160-171. DOI: 10.1016/j.jcis.2018.01.028
- [82] Shi S, Deng T, Zhang M, Yang G. Fast facile synthesis of SnO<sub>2</sub>/graphene composite assisted by microwave as anode material for lithium-ion batteries. *Electrochimica Acta*. 2017;**246**:1104-1111. DOI: 10.1016/j.electacta.2017.06.111
- [83] Dursun B, Topac E, Alibeyli R, Ata A, Ozturk O, Demir-Cakan R. Fast microwave synthesis of SnO<sub>2</sub>@graphene/N-doped carbons as anode materials in sodium ion batteries. *Journal of Alloys and Compounds*. 2017;**728**:1305-1314. DOI: 10.1016/j.jallcom.2017.09.081
- [84] Wang N, Goh QS, Lee PL, Magdassi S, Long Y. One-step hydrothermal synthesis of rare earth/W-codoped VO<sub>2</sub> nanoparticles: Reduced phase transition temperature and improved thermochromic properties. *Journal of Alloys and Compounds*. 2017;**711**:222-228. DOI: 10.1016/j.jallcom.2017.04.012
- [85] Wang N, Duchamp M, Dunin-Borkowski RE, Liu S, Zeng X, Cao X, Long Y. Terbium-doped VO<sub>2</sub> thin films: Reduced phase transition temperature and largely enhanced luminous transmittance. *Langmuir*. 2016;**32**:759-764. DOI: 10.1021/acs.langmuir.5b04212
- [86] Wang N, Duchamp M, Xue C, Dunin-Borkowski RE, Liu G, Long Y. Single-crystalline W-doped VO<sub>2</sub> nanobeams with highly reversible electrical and plasmonic responses near room temperature. *Advanced Materials Interfaces*. 2016;**3**:1600164. DOI: 10.1002/admi.201600164
- [87] Wang N, Liu S, Zeng XT, Magdassi S, Long Y. Mg/W-codoped vanadium dioxide thin films with enhanced visible transmittance and low phase transition temperature. *Journal of Materials Chemistry C*. 2015;**3**:6771-6777. DOI: 10.1039/c5tc01062d
- [88] Mounasamy V, Mani GK, Ponnusamy D, Tsuchiya K, Prasad AK, Madanagurusamy S. Template-free synthesis of vanadium sesquioxide (V<sub>2</sub>O<sub>3</sub>) nanosheets and their room-temperature sensing performance. *Journal of Materials Chemistry A*. 2018;**6**:6402-6413. DOI: 10.1039/c7ta10159g
- [89] Alexeev AM, Barnes MD, Nagareddy VK, Craciun MF, Wright CD. A simple process for the fabrication of large-area CVD graphene based devices via selective in situ functionalization and patterning. *2d Materials*. 2017;**4**:011010. DOI: 10.1088/2053-1583/4/1/011010
- [90] Yang Y, Lee K, Zobel M, Mackovic M, Unruh T, Spiecker E, Schmuki P. Formation of highly ordered VO<sub>2</sub> nanotubular/nanoporous layers and their supercooling effect in phase transitions. *Advanced Materials*. 2012;**24**:1571-1575. DOI: 10.1002/adma.201200073